

Analysis of Pilot Contamination in Very Large Scale MIMO Systems



By

Zaka ul Mulk

NUST201260894MSEEC61212F

Supervisor

Dr. Syed Ali Hassan

Department of Electrical Engineering

A thesis submitted in partial fulfillment of the requirements for the degree
of Masters in Electrical Engineering (MS EE-TCN)

In

School of Electrical Engineering and Computer Science,
National University of Sciences and Technology (NUST),

Islamabad, Pakistan.

(April 2015)

Approval

It is certified that the contents and form of the thesis entitled “**Analysis of Pilot Contamination in Very Large Scale MIMO Systems**” submitted by **Zaka ul Mulk** have been found satisfactory for the requirement of the degree.

Advisor: Dr. Syed Ali Hassan

Signature: _____

Date: _____

Committee Member 1: **Dr. Adnan Kiani**

Signature: _____

Date: _____

Committee Member 2: **Dr. Khawar Khurshid**

Signature: _____

Date: _____

Committee Member 3: **Dr. Hassaan Khaliq**

Signature: _____

Date: _____

Dedication

I dedicate this thesis to my parents.

Certificate of Originality

I hereby declare that this submission is my own work and to the best of my knowledge it contains no materials previously published or written by another person, nor material which to a substantial extent has been accepted for the award of any degree or diploma at NUST SEECS or at any other educational institute, except where due acknowledgement has been made in the thesis. Any contribution made to the research by others, with whom I have worked at NUST SEECS or elsewhere, is explicitly acknowledged in the thesis.

I also declare that the intellectual content of this thesis is the product of my own work, except for the assistance from others in the project's design and conception or in style, presentation and linguistics which has been acknowledged.

Author Name: **Zaka ul Mulk**

Signature: _____

Acknowledgment

All praises to Allah Almighty who gave me strength to complete this work. I would like to thank my adviser who made this research work possible. I have achieved this goal only because of his guidance and motivation.

Zaka ul Mulk

Table of Contents

1	Introduction	1
1.1	Background	3
1.2	Going Large: Massive MIMO	6
1.3	The potential of Massive MIMO	8
1.4	Limiting factors of massive MIMO	9
1.4.1	Channel Reciprocity	9
1.4.2	Pilot Contamination	10
1.4.3	Orthogonality of Channel Responses and Radio Propagation	13
1.5	Thesis Contribution	14
1.6	Thesis Organization	15
2	Literature Review	16
2.1	Pilot Open-Loop Power Control	18
2.2	Less Aggressive pilot Reuse	21
2.3	Effect of pilot Contamination in massive MIMO cellular uplink systems with pilot reuse	24
3	System Model	27

<i>TABLE OF CONTENTS</i>	vii
3.1 Multi-cell Uplink Communication	29
3.1.1 Uplink Training with Pilot Reuse	29
3.1.2 Actual Transmission of Data	31
3.1.3 Achievable Cell Throughput	31
4 Numerical Results	36
5 Conclusion	43

List of Figures

1.1	Deployment and configuration of massive MIMO antenna arrays.	7
1.2	Pilot Contamination for uplink transmission.	12
1.3	Array of Massive MIMO antennas used for the measurements.	14
2.1	Uplink transmission with all users transmitting at max power	20
2.2	Time-frequency resources consumed by pilots for $K = 12$, reuse factor 1 and 1/3 respectively	22
2.3	Pilot distribution scheme for Soft pilot Reuse	24
2.4	Network topology for pilot reuse in uplink cellular system. . .	26
3.1	System model	28
4.1	Average throughput with different number of users and reuse factor	37
4.2	Average throughput with different number of antennas	38
4.3	Average throughput with coherence period and different number of users	39
4.4	Interference types with reuse factor and different number of users	40
4.5	Comparison between throughputs of MMSE and MRC receivers	42

List of Abbreviations

Abbreviation	Description
BS	Base Station
MIMO	Multiple Input Multiple Output
MU-MIMO	Multi User-Multiple Input Multiple Output
TDD	Time Division Duplex
FDD	Frequency Division Duplex
SINR	Signal-to-Interference Plus Noise Ratio
SDMA	Space Division Multiple Access
CSI	Channel State Information
MRC	Maximum Ratio Combining

Abstract

In this thesis, a regular hexagonal geometry with random deployment of users is considered in order to study the impact of pilot contamination for a more general scenario. Specifically, we study a conventional frequency reuse hexagonal geometry and derive the throughput of the network when multiple users are reusing the same pilots leading to pilot contamination problem. We restrict ourselves to only first tier of co-channel interferers. Finally, with the help of numerical simulations, relations among cell throughput, numbers of antennas, number of users per cell, pilot reuse factor and coherence period have been studied. It is shown that the reuse pattern has strong impact on the system achievable throughput.

Chapter 1

Introduction

From the past ten years, the wireless technology has been made the constitutional supporter of universal and flexible network access. There is a requirement of easy connectivity and data rates due to which the developments in cellular technology are being made very fast. A host of data demanding applications is needed to be fulfilled, which are lead by video streaming, navigation and graphics heavy social media boundaries on portable gadgets. For attaining high rates and ethereal effectiveness in wireless communication systems, MIMO i.e. Multi-input multiple-output has come out as the part of major technologies from about past ten years. MIMO air interface is being counted on, by the newest wireless transmission principles, through which cost-effective consumption of gigabit links in wireless local area network in addition to commercial cellular networks are gained. Attainments through MIMO, on the other hand, are acquired at the rate of amplified processing density and hardware costs. In the previous ten years, by assisting large-scale creation of low-cost chips with small form features, hardware technology have acted as facilitator for MIMO due to their fast progresses. 8 antenna ports

at base station and equivalent amount of ports at terminal are acceptable in the recent state of art in cellular technology. Development of massive MIMO is a result of the struggles being made through research, to form a technology which will raise spectral efficiency while the mass of processing complexity is controlled at the BS.

There are many advantages of Multi-user MIMO over general point-to-point MIMO for example the antenna terminals needed are often cheap, the environment required is not supposed to be rich in scattering and the allocation of resources is simplified as the time-frequency bins are utilized by every active terminal. However, using almost equal terminals and number of antennas multi-user MIMO is not a scalable technology. Massive MIMO which is also known as Very Large MIMO, Large-Scale Antenna Systems and Hyper MIMO has a clear edge over the technology that is currently in practice by using a large number TDD operations and service antennas on terminals [1][2][3]. With the help of extra antennas throughput and radiated energy efficiency can be improved at a large scale. A lot of other benefits of massive MIMO include the reduced latency, robustness, simplified MAC layer and utilization of cheap low power components. The throughput is mainly dependent upon the propagation environment when the channels assigned to the terminals are orthogonal. However, no limitations have been disclosed in this regard with the help of experiments. Therefore massive MIMO invokes many research problems which need to be addressed yet including internal power consumption, increasing energy efficiency, making of low cost components and their synchronization issues.

1.1 Background

Interference initiated by other appliances broadcasting at the same time over the same bandwidth and fading or the difference of signal power over time, are the two foremost troubles confronted by the wireless communication of given bandwidth. Signals are disturbed to SINR i.e. signal-to-interference-and-noise ratio at the receiver by these sources and a crucial edge is located on the attainable rate with a randomly low error rate.

To enhance linearly with the bandwidth and logarithmically with SINR, R is demonstrated, if Gaussian allocation of thermal noise and interference power occurs. The spectral efficiency of a link is referred to as the information rate which is diffused in one unit bandwidth. While positioning a cellular system, the most important metric to bear in mind is spectral efficiency, because spectrum is a restricted and costly supply. Only adequate achievements in the spectral efficiency of the link may be achieved as an outcome of a huge growth in signal power because spectral efficiency only develops logarithmically with SINR. Additionally, the interference initiated on other links rise comparably as the signal power rises, and the enhancement of spectral efficiency of the overall system is restricted. Alternate ways to advance the spectral efficiency are obviously required, either by interference reduction or by formation of extra orthogonal channels within the given spectrum.

To upgrade spectral efficiency, MIMO uses the basic method; (i) to enhance the collected signal power, signals are administered comprehensibly at multiple transmitter ports, (ii) Termination of interference, or (iii) individual data streams diffused over spatially separate links. These are corresponding methods, and there are several factors responsible for the optimal attempt

with regard to maximizing R . To convey/ accept data to/from each terminal spatially detached streams can be used in such a situation where the mass of UEs over the same time-frequency resources, is assisted by BS. Above mentioned method is called MIMO (MU-MIMO), similarly referred to as space division multiple access (SDMA). With the number of terminals provided under the standard channel circumstances, spectral efficiency of MU-MIMO can multiply linearly, with surplus degrees of independence at the BS array.

Honestly exact data of the forward and reverse-link channels for each terminal is needed by the BS to attain profits in R with MU-MIMO. Diffusing an identified arrangement of symbols (pilot sequence) and observing the outcome which marks effect on the channel arrangement at the receiver is a general method used for assessing channel. The channel assessment is only beneficial for a restricted phase of time and coherence interval; the channel can be supposed persistent over the coherence frequency interval. The amount of supplies accessible for collecting or diffusing data within the coherence interval is restricted due to the amount of supplies used to acquire the channel state information (CSI), therefore, attaining CSI comprises an operating cost. The arrangement to conclude the optimal considerations among pilot and data revenues for amplifying the cell amount is a significant research dilemma.

The signal is concentrated into smaller sections of space at the preferred terminal due to the accumulation of more antennas at BS, as a result, the collected signal power and vindicating interference is enhanced. The inquiry of asymptotically immeasurable amount of antennas at the BS in a multi-cell structure, and its influence on the R is assessed by this inspiration. It

has been discovered that the system material and energy productivity is being improved intensely in case of noticeably many antennas. Simple lined administering evaporates the result of disturbing sound and interference, and as an outcome of pilots being reprocessed across cells, impurity of channel assessment limits the operating supposedly.

In wireless communication systems multiple antennas are used to transmit multiple streams of data simultaneously in MIMO technology. Multi user MIMO is a term used when MIMO communicates with more than one terminal at a single time. Following are the main advantages provided by the MU-MIMO:

- *Improved energy efficiency*, energy is only transmitted in a direction where the terminal is located hence emitted energy can be focused into the spatial directions
- *Increased data rate*, with the help of multi antennas more data streams can be sent hence more terminals can be served.
- *Enhanced reliability*, more antennas more paths hence the probability of a signal to reach its destination is increased.
- *Reduced interference*, the direction for the transmission of a signal is controlled at the base station hence interference can be avoided. MU-MIMO is evolving the broadband standards of wireless i.e. 4G LTE and LTE-Advance (LTE-A). In recent years this technology is getting matured very rapidly. If we consider the above four points than we know the fact that with the increase in number of antennas we can achieve better results in all of them, but the number of antennas used

today is modest. Maximum number of antennas allowed by LTE-A is 8 and equipments being built dont even have this amount of ports in the base station.

1.2 Going Large: Massive MIMO

Massive MIMO is the evolution of MU-MIMO that massively scales up the magnitude of MIMO. In the same time frequency resource tens of terminals are considered to be served with hundreds of base station antennas [4]. Basically massive MIMO will provide all the benefits of conventional MU-MIMO but at a very large scale. Massive MIMO is a technology of future that will provide broadband networks more security, robustness, energy efficiency and efficient use of spectrum. Different kinds of deployment and configuration for massive MIMO can be envisioned in the Fig 1.

Massive MIMO requires good knowledge about the channel for both uplink and downlink channels for the fact that it uses spatial multiplexing. This can be easily achieved in uplink when terminals send pilots to the base station that can be used to estimate the channel. In the downlink it is more complex. First base station sends pilots to the terminals where they estimate the channel and quantize the so-obtained estimation; this estimation is then sent back to the base station. This is not possible in massive MIMO because of two reasons. First, the downlink pilots should be orthogonal which means that as the number of antennas increase more frequency and time resources are utilized than conventional MIMO [5]. Secondly, each terminal accepts multiple numbers of pilots so the number of channel estimation at the termi-

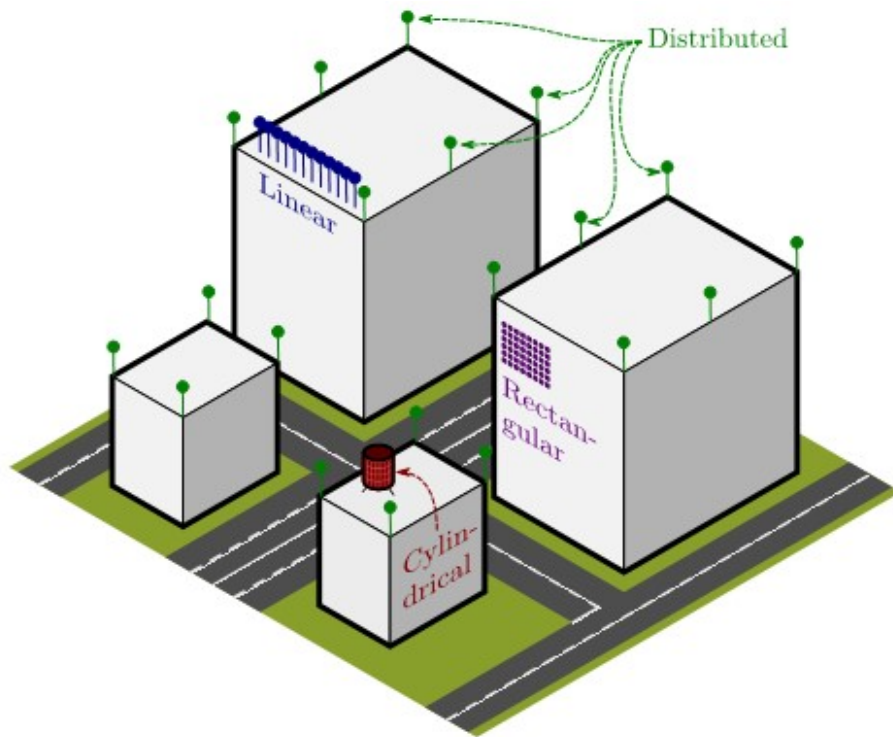


Figure 1.1: Deployment and configuration of massive MIMO antenna arrays.

nal also increase with the increase in number of antennas. The solution for this problem is to operate in TDD mode and depend upon the uplink and downlink channel reciprocity [6].

1.3 The potential of Massive MIMO

Some of the major benefits of massive MIMO are:

- Increase in capacity and energy efficiency, with the help of spatial multiplexing we can increase the capacity up to 10 times than the conventional MIMO [7]. The reason is that many tens of terminals are served in the same frequency and time resource hence increasing the spectral efficiency as well. By focusing our energy with extreme sharpness we can into small areas we can increase energy up to 100 times.
- Massive MIMO can be built with cheap components; the ultra linear 50 Watt amplifiers are replaced by the cheap hundreds of amplifiers that has the output power in milli-Watt range. Massive MIMO rely on the law of large numbers which concludes that the fading, noise and hardware imperfections cancel out when signals are transmitted from many antennas. This will help a lot in the near future as the energy issues faced by the base stations are getting severe day by day. Massive MIMO decreases the energy consumption by the order of 2 as compared to the conventional MIMO.
- Massive MIMO offers significantly less latency, as discussed earlier massive MIMO depends upon the weak law of large numbers which cancels out the fading and noise effects.

- Simplification in the multiple access layer, when using OFDM almost same channel gain is provided to each subcarrier so whole bandwidth can be given to all the subcarriers.
- Massive MIMO has robustness against jamming, in massive MIMO this is achieved by spreading the data in frequency domain that it makes it difficult to decode.

1.4 Limiting factors of massive MIMO

A lot of research is being carried out in this domain still there are many open research problems that are to be solved yet. Mainly these problems include:

1. Channel Reciprocity.
2. Pilot Contamination.
3. Orthogonality of Channel Responses and Radio Propagation.

1.4.1 Channel Reciprocity

Channel reciprocity is what TDD operation depends upon [8]. Propagation channel is believed to be essentially reciprocal, only if the propagation is not affected by materials having unusual magnetic properties. Yet, it is possible that the hardware chain in the base station and terminal transceivers are not reciprocal between the uplink and the downlink. Adjustment of the hardware chains does not apparently create any serious problem and there are such calibration-based solutions which have been tested to a certain degree [9, 10]. Specially, [9] handles reciprocity calibration for 64-antenna system with more

specifications and affirm a successful experimental application. It is to be noted that, in order to acquire a full beamforming benefits of massive MIMO, calibration of the terminal uplink and downlink chains is not compulsory; a coherent beam will surely be passed to the terminal by the arrays, only if the base station equipment is accurately calibrated (some imbalance will still be possible in terminals receiver chain but by transmitting pilots to the terminal through the beams, it is possible to handle this imbalance). Complete calibration in array is not necessary. One of the antennas can rather be handled as a reference and hence the signals can be exchanged from the reference antenna to the other antennas to derive a settlement factor between the antennas, which is suggested in [9]. It can also be possible to abandon the reciprocity calibration in the array, for instance, supposing that the maximum phase difference between the uplinks and the downlinks were less than 60 degrees, coherent beam forming would still exist (at least with MRT beamforming) even with a possible 3db reduction in gain.

1.4.2 Pilot Contamination

The uplink pilot sequence that is ideally assigned to any terminal in massive MIMO systems is orthogonal [11]. Therefore, number of pilots required in a system is upper bounded and are defined as the division of channel coherence time by channel delay spread. In a general scenario the number of maximum orthogonal pilots for 1 millisecond coherence time is estimated to be 200 [12]. In a multi cellular system these pilots are used very quickly that demands the need of reuse of pilots [13][14]. Pilot contamination is the term associated with the negative effects of reusing pilots in more than one cells

[15]. Correlation of pilot sequence assigned to a particular terminal with the received pilot signal gives the estimation of channel that is contaminated by channels that use the same pilot sequence. Therefore considering downlink beamforming interference occurs in those terminals that have the same pilot sequence similar is the case for uplink transmissions. This interference increases directly with the increase in service antennas [16]. Pilot contamination is not only restricted to massive MIMO it is a general phenomenon but it appears at a high rate in massive MIMOs than ordinary MIMOs [17]. Marzetta et al. [18] has discussed in their work that the occurrence of pilot contamination degrades the performance. There are several ways that can be used in order to avoid this contamination as the channel estimation is dependent upon it in many cases.

- One way is to use less number of reuse factor for pilots which sets the cells with same pilot sequence far apart. Or the allocation of pilots can be done adaptively but so far optimal scheme is not known.
- Blind techniques and channel estimation algorithms are also used to eliminate the effect of interference.
- Using precoding techniques that involve the network topology like pilot contamination techniques [19]. This utilizes the cooperative communication over multiple cells that are outside the beamforming region in order to at least remove the effect of partially overlapping interference caused by pilot contamination. This kind of precoding does not require

the actual estimate of channel instead it only requires the slow fading coefficients. In practical these precoding techniques need to be developed yet.

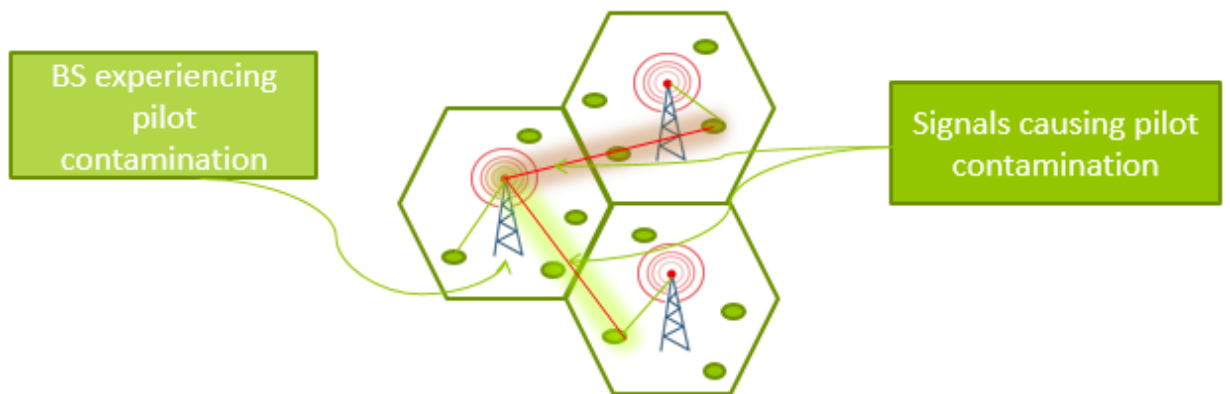


Figure 1.2: Pilot Contamination for uplink transmission.

1.4.3 Orthogonality of Channel Responses and Radio Propagation

Massive MIMO (Specifically MRC/MRT processing) depends to a great degree on Favorable Propagation which is a quality of the radio environment [20]. In simple words, favorable propagation means that the propagation channel feedbacks from the base station given to several terminals are different enough. Channel assessments should be done with the help of realistic antenna arrays, in order to study the nature of massive MIMO systems. It is done this way because if using large arrays, channel behavior changes from what is mostly seen with the use of conventional smaller arrays. These are the most crucial differences; (I) a large scale fading is possible over the array and (II) perhaps the small-scale signal statistics change as well over the array [21]. It is also appropriate for arrays which are smaller in size with directional antenna elements pointing in different paths [22].

Two massive MIMO arrays which are used for the measurement reported in the paper are shown in Figure.5. A closely packed round massive MIMO array with 128 antenna ports is at the left side. This array constitutes 16 dual-polarized patch antenna elements in spheres, and 4 of these spheres are stacked on one and other. This array gives the possibility to settle down the scatters at various elevations along with the benefit of being closely packed. But because of its defined aperture, it deals with worse settlements in azimuth. At the right side there is a larger in size straight horizontal array, where, to imitate a genuine array with same proportions, a single omnidirectional antenna element is moved to 128 various locations in an otherwise constant environment [23].



Figure 1.3: Array of Massive MIMO antennas used for the measurements.

1.5 Thesis Contribution

In this thesis, a regular hexagonal geometry with random deployment of users is considered in order to study the impact of pilot contamination for a more general scenario. Specifically, we study a conventional frequency reuse hex geometry and derive the throughput of the network when multiple users are reusing the same pilots leading to pilot contamination problem. We restrict ourselves to only first tier of co-channel interferers. Finally, with the help of numerical simulations, relations among cell throughput, numbers of antennas, number of users per cell, pilot reuse factor and coherence period have been studied. It is shown that the reuse pattern has strong impact on the system achievable throughput.

The concept of massive MIMO includes a large array of transmit antennas i.e. up to hundreds of antennas at the base station. It has been concluded in this thesis that massive MIMOs can be a lot helpful in improving the data rates and link reliability. Moreover powers saving issues are also solved with the help of this concept. Massive MIMO which is also known as Very Large MIMO, Large-Scale Antenna Systems and Hyper MIMO has a clear edge

over the technology that is currently in practice by using a large number of TDD operations and service antennas on terminals . With the help of extra antennas throughput and radiated energy efficiency can be improved at a large scale

1.6 Thesis Organization

In Chapter 2 we describe the literature review related to the massive MIMO systems and pilot contamination. Different techniques have been studied to analyze the effect of pilot contamination and techniques related to mitigate the effect of pilot contamination have also been studied. In Chapter 3 System Model for the throughput of the hexagonal geometry and random deployment of users has been described. All the mathematical equations have been thoroughly explained with derivations in this chapter. In Chapter 4 Numerical Results have been discussed. All the figures have been plotted on Matlab with respect to different parameters like throughput, reuse factor, number of users per cell and coherence time. Chapter 5 contains the Conclusion of the thesis and the future work. References have been given at the end.

Chapter 2

Literature Review

In wireless cellular systems, multiple antennas are used at the base station (BS), which provide high throughput as well as improved quality of service to its users. Considering a multiple cell geometry, where each cell is equipped with tens of antenna making a massive MIMO system, it is obvious that the knowledge of channel state information (CSI) at the base station plays an important role to achieve high system performance. The most efficient way of obtaining CSI is through reciprocity that uses uplink training of pilots [24], [25]. The major constraint while considering a multiple cell scenario is the allocation of pilot signals to the users. This affects the system performance in a great way as the CSI is further dependent upon the pilot allocation scheme. The frequent mobility of users shortens the channel coherence period and as a result the length of pilot sequence gets limited. Therefore, considering the scarcity of bandwidth it is not feasible to allocate distinct orthogonal pilot signals to users in each cell. The major issue of reusing non-orthogonal pilot signals in different cells is commonly known as pilot contamination that limits the achievable throughput [26]. It is caused when the CSI at BS is corrupted

because of pilot signals from neighboring cells using the same frequency.

Marzetta [18] has shown in his work that as the number of antennas increases to infinity, the throughput eventually saturates. Gopalakrishnan et al. [27] and Ngo et al. [28] derived the asymptotic throughput bound, which shows that the throughput is limited by pilot contamination. Different techniques have been studied in order to reduce the effect of pilot contamination. Tadilo et al. [29] proposed a novel pilot optimization and channel estimation algorithm to reduce the weighted sum mean square error (WSMSE). Papadopoulos et al. [30] and Huh et al. [31] improved the throughput with the help of cooperative communication in which they divided the mobile terminals in different groups. Appaiah et al. [32] used asynchronous transmission of pilots to reduce the correlation error for channel estimation and Jose et al. [26] worked on regularized zero force precoding. Peng Xu et al. [33] studied that the pilot contamination problem is not relieved by increasing number of pilot sub-carriers while using the channel estimators like least square (LS) and minimum mean square error (MMSE) but it can be mitigated if proper pilot reuse or allocation scheme is proposed [34][35]. Yang et al. [36] derived the throughput for a line geometry of cells where users are co-located in each cell.

In massive MIMO system, the pilot resources are constructed in a way that theyd be orthogonal in the cell, but are used again by terminals in other cells. Pilot contamination is the reuse of pilots in neighboring cells causes intrusion during channel estimation phase. Different techniques have been studied to mitigate the effect of pilot contamination. Some of them have been explained below in detail

2.1 Pilot Open-Loop Power Control

Mobile terminals pathloss and transmit power are what the average obtained power of a pilot signal at the BS relies on. Moreover, a terminal has normally a lower pathloss, if its placed near the BS, and therefore, if located at the BS it would have higher signal power. If terminals are at cell-edge they normally have greater pathloss, and hence, even during transmitting at their maximum power, they have a low signal power. This is why they are prone to disturbance from non-orthogonal pilot transmissions from the cells nearby. On the contrary, when the terminals are near BS, they enjoy a reduced pathloss, which in return gives a better SINR.

Uplink power control or disseminating the power control in the reverse link is very essential in controlling the shared radio resources. Pilot open loop power control (pilot OLPC) scheme approves the terminal to adapt the transmit power of its pilot signal based on its approximate of the pathloss to its serving BS. The pathloss is estimated from forward-link reference signal by the terminals which try to duplicate network-wide desired pilot signal strength at the BS. The received pilot SNR is balanced by this technique at the serving BS of a terminal with the interruption produced at the nearby BSs [37]. SNR fairness of pilot signals is maximized by the attempts of Pilot OLPC, through compensating for their further added pathloss. Pathloss compensation has the planned effect of shortening overall pilot intrusions in the network at the price of SNR deterioration for terminals positioned near BS.

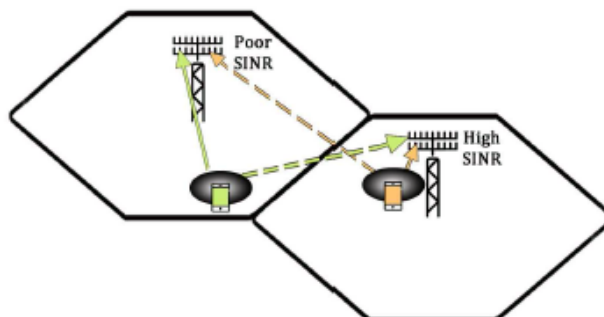
While using closed-loop power control technique the BS transmits periodic signals for power increment or decrement based on the estimates from

SINR due to which tighter range of operating point is created. We can implement power control with an ease because it only depends upon large-scale fading [38]. The compensation factor and operating levels depend upon the existing standard measurements. Here, only open loop closed systems transmit power will be considered. The transmit power will depend upon two things (i) an open-loop path loss compensation factor and (ii) a base level of power P_0 that is same across the system. The pathloss β_{jk} for the k^{th} terminal of j^{th} cell is given as

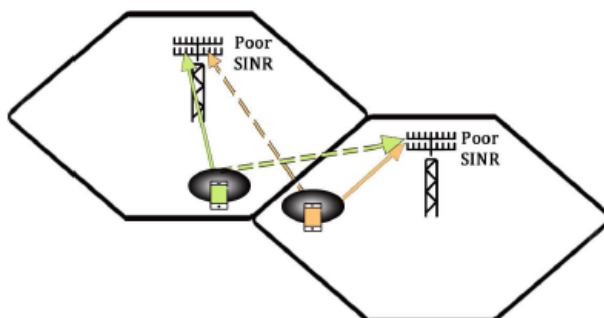
$$P_{jk} = \min(P_0 + \alpha \cdot \beta_{jk}, P_{max}) + 10\log_{10}M \quad (2.1)$$

Where α is the path loss compensation component, P_{max} is the maximum terminal power in a single RB and M is the total number of RBs allocated. Maximum fairness for the edge users is achieved when $\alpha =$ *i.e. full path loss compensation*.

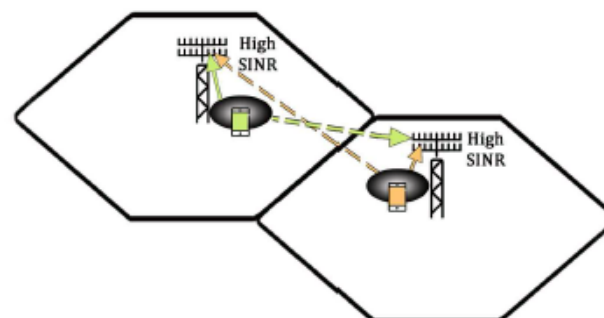
In the presence of OLPC the users that have strong channel estimates control their transmit power in order to reduce the SNR to achieve the desired level of SNR. By doing so, the interference created on other BS is also reduced by the same amount. The users at the cell edge continue to transmit at the higher power that improves their SINR as described in Fig 2.1a. Whereas, the SINR of the user closer the base station is decreased because of OLPC. The SINR of a received signal depends upon the estimate of channel at the BS. Per-cell throughput is increased if estimated channel is good enough with the help spatial multiplexing [39][40]. The achievable throughput in a multi-cell scenario depends upon the operating point and the amount of users and their location in a cell [41].



(a) Pilot reuse at cell edge and close to BS



(b) Pilot reuse by close cell-edge terminals



(c) Pilot reuse close to serving BSs

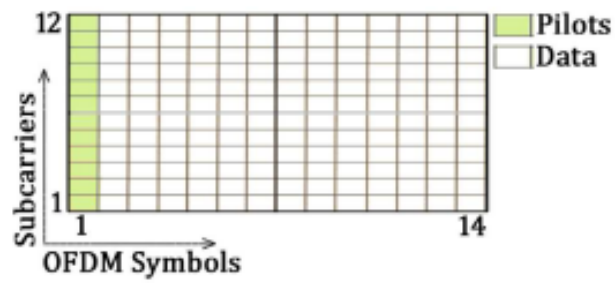
Figure 2.1: Uplink transmission with all users transmitting at max power

2.2 Less Aggressive pilot Reuse

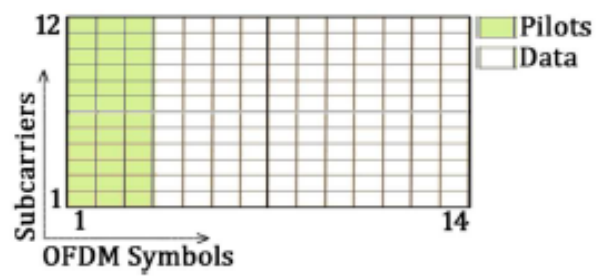
Full pilot reuse prompts most extreme inter-cell interference amid channel estimation, which can be relieved utilizing a less forceful pilot reuse factor. Pilot reuse is closely resembling to the conventional frequency reuse as the terminals inside the pilot reuse region can use just a small amount of the time-frequency resources, within the channel estimation stage. Whereas, in the case of pilot reuse, every terminal is allowed to utilize all the accessible resources for communication for the remaining coherence time. The pilots are reused in the system by the rate of $1/U$, where U is the quantity of cells that are allotted orthogonal pilots. While using reuse factor of $U \geq 1$ dependably limits the effect of pilot contamination by allocating orthogonal pilots to the neighboring cells. The aggregate number of novel time-frequency components held for pilot transmission are KU , where K is the quantity of terminals in each cell.

The trifling instance of pilot reuse is full pilot reuse with $U = 1$. For this situation, we hold K time-frequency indices for pilot sequences. The indices may be found anyplace inside the resource block without loss of simplification. We create K orthogonal pilot sequences including these indices, that are circulated at arbitrary or algorithmically among the mobile user inside each one cell. Since the cells are thought to be synchronized, the pilot transmissions are synchronized crosswise over cells also.

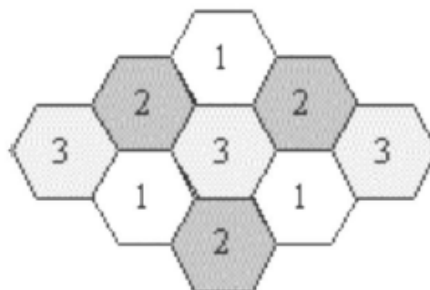
Moderate value of Reuse factor in this scenario will be used and the orthogonal pilots are used by the terminals of the nearby cells that cause much interference. If we use a hexagonal geometry for cellular layout then the minimum reuse factor that can help in assigning the orthogonal pilots to



(a) Pilot reuse 1



(b) Pilot reuse 1/3



(c) Pilot reuse 1/3 pattern

Figure 2.2: Time-frequency resources consumed by pilots for $K = 12$, reuse factor 1 and $1/3$ respectively

the adjacent cells will $1/3$. The resources used to implement this reuse factor will be three times the number of users i.e. $3K$. A group of pilots is assigned to each cell and the terminals are assigned with the pilots as in the case of full pilot reuse scheme. In a similar way we can define schemes for the reuse factors 4, 7 and 9 which can reduce the pilot contamination even more as the terminals using the same pilots are now placed at a farther distance.

Using higher values of pilot reuse we can eliminate the pilot contamination but at the cost of the overheads added by using the pilot resources. This overhead will limit the amount of data that is to be sent in the next phase. Anyhow this better estimate of channel will result in better beamforming for the uplink and downlink transmissions using spatial multiplexing to serve the terminals. Hence there is a tradeoff between the exact beamforming and data transmission afterwards.

There is another technique that is also known as *Soft Pilot Reuse*, in which the terminals at the cell edge of each cell are assigned the orthogonal pilot sequences. Hence the terminals will not affect the transmission of the adjacent cell terminals with this implementation. As we know that cell-edge terminals have the poor SNR therefore with the help of this technique higher rates can also be achieved.

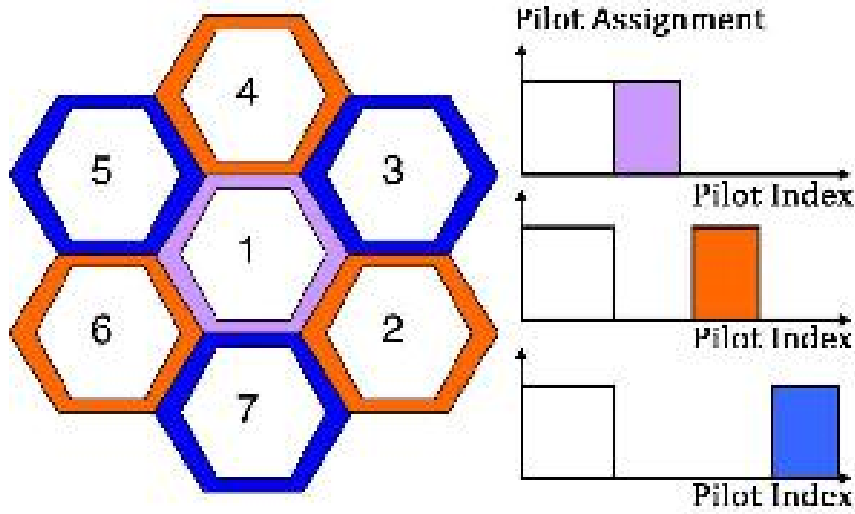


Figure 2.3: Pilot distribution scheme for Soft pilot Reuse

2.3 Effect of pilot Contamination in massive MIMO cellular uplink systems with pilot reuse

A pilot reuse scheme has been employed in an uplink massive MIMO system. Lower bound for non asymptotic throughput is shown to be precise with the help of simulations. Three types of interferences affect the lower bound namely: inter-cell interference, intra-cell interference and pilot contamination. Certain conditions are examined on which the behavior of each interference dominates. These conditions include the pilot reuse number, M (number of mobile stations) and network topology. For example when $M=100$ then throughput is maximum when we use pilot reuse number 2. Pilot contamination in this case is eliminated and inter-cell interference dominates.

In this paper a pilot reuse scheme is considered for an uplink massive

MIMO network. Pilot reuse number can be more than one in this case. Lower bound for throughput that is non-asymptotic is derived for the cellular network. The lower bound is characterized with three interference terms: inter-cell, intra-cell interference and pilot contamination. Studies on the conditions for which certain interference dominates are discussed with the help of numerical simulations which gives insight about the relation among number of base station antennas optimal throughput, network topology and pilot reuse number.

A $2L+1$ cells ranging from L to L are considered to be deployed in a line, shown in the following figure. M numbers of base station antennas are located in each cell and the distance between two closest neighboring base stations is d . k number mobiles are served in each cell. The K mobiles are considered to be single antenna and co-located for the sake of simplicity i.e. the distance between mobile and its respective base station is d_0 .

In this paper lower bound for throughput in a massive MIMO uplink cellular network with a pilot reuse scheme has been found. Three types of interference were identified and discussed. It has been shown that the pilot contamination does not limit the throughput when (1) pilot reuse number is greater than 1 or (2) the mobiles are located at the cell center with pilot reuse 1.

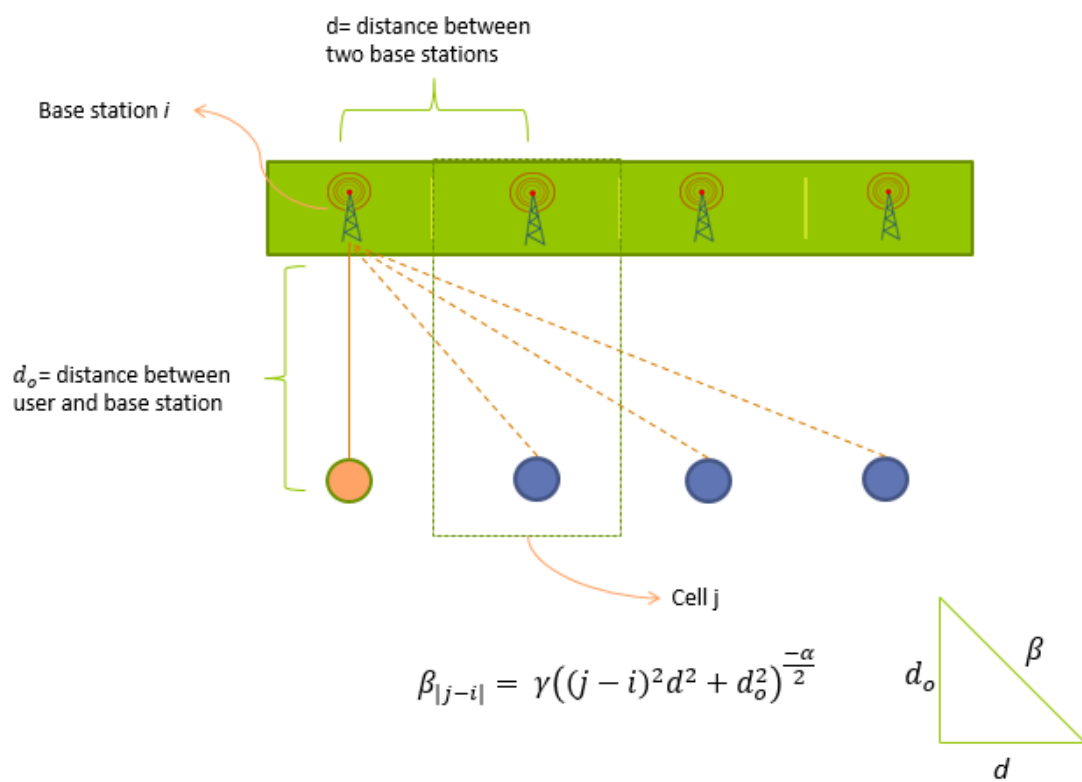


Figure 2.4: Network topology for pilot reuse in uplink cellular system.

Chapter 3

System Model

Consider a tier-1 hexagonal geometry of a cellular system, where each cell has a radius R . By tier-1 we refer to the area of interfering cells that causes co-channel interference (CCI) and is considered the main source of pilot contamination. The reuse factor of the hexagonal geometry is given by Q , where $Q = \{1, 3, 4, 7, \dots\}$. For instance, in Fig. 1, six interfering cells for the center cell constitute tier-1 geometry with $Q=1$. Each cell contains an M -antenna base station (BS) that serves K randomly deployed single antenna mobiles. Let $d_{i,j,k}$ be the distance between user k of cell j and the BS antennas of cell i , then the path loss factor is given by

$$\varphi_{i,j,k} = \frac{1}{d_{i,j,k}^\alpha} \quad (3.1)$$

Where α is the path loss exponent. Although the distance to all BS antennas potentially remains the same for one user, however, we will use this notation for consistency with fading gains.

A Rayleigh block fading channel is assumed where all the channel co-

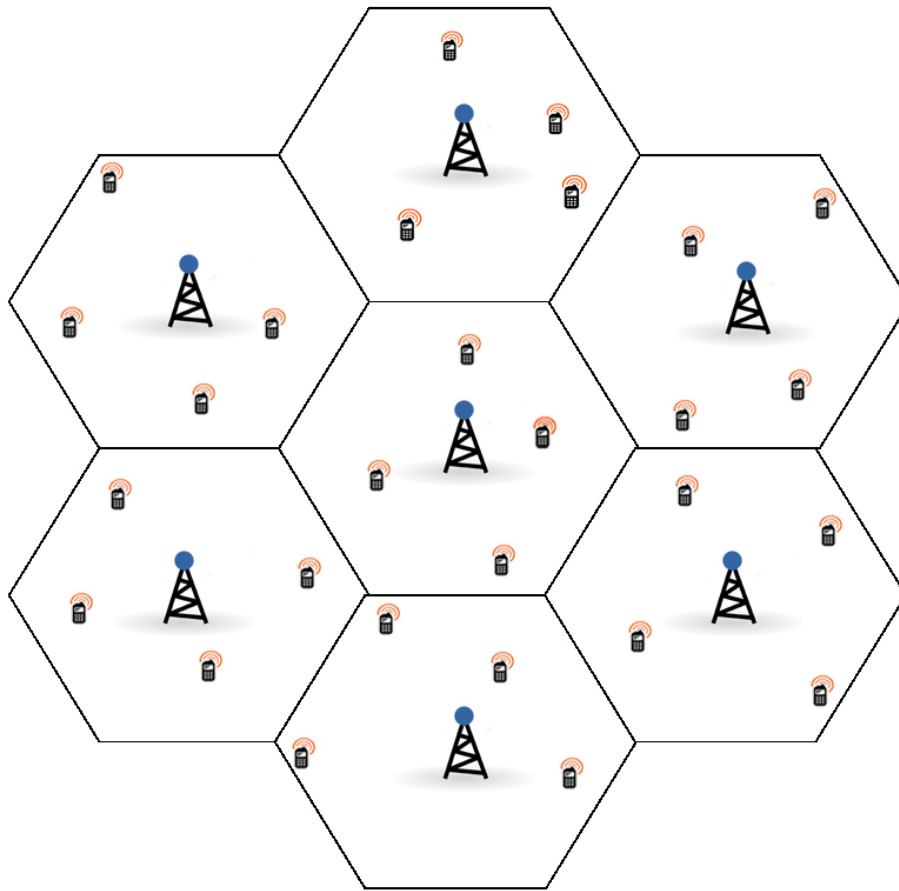


Figure 3.1: System model

efficients remain constant for a block of T symbols; T being the channel coherence period. Considering the geometry, the channel matrix between the antenna i and mobiles in cell j is $\mathbf{C}_{i,j} \in \mathbb{C}^{M \times K}$ where all the entries of $\mathbf{C}_{i,j}$ are independent and identically distributed (i.i.d.) complex Gaussian with zero mean and unit variance.

3.1 Multi-cell Uplink Communication

All the mobiles in this uplink scenario communicate with their respective base station in two stages: uplink training with pilot reuse and actual transmission of the data.

3.1.1 Uplink Training with Pilot Reuse

In each cell, orthogonal pilots are assigned to the users, which are reused by other cells by the factor Q . Assume a pre-designed pilot sequence matrix

$$\mathbf{\Psi} = [\Psi_0, \dots, \Psi_{Q-1}] \in \mathbb{C}^{QK \times QK} \quad (3.2)$$

Where $\mathbf{\Psi}$ is divided among all cells. Assume that Ψ_0 is assigned to the Cell 0 which is considered to be the serving cell (center cell from Fig. 1) and the pilot sequence is further reused by Cell lQ where $1 \leq |l| \leq \lfloor \frac{L}{Q} \rfloor$ where L is the total number of cells in geometry. The pilot $\Psi_{q,k}$ is assigned to a single user k of a cell in order to remove intra-cell interference with the help of orthogonality of pilot signals.

We only analyze Cell 0 here for brevity. In a single time-frequency block, all the mobiles send their pilot signals to the base station. The signals received at base station 0 are

$$\mathbf{P}_0 = \sqrt{\phi_\tau QK} \sum_{j=0}^{L-1} \mathbf{C}_{0,j} \Psi_{(j)}^* + \mathbf{W}_0, \quad \in \mathbb{C}^{M \times K} \quad (3.3)$$

where $\mathbf{C}_{0,j} = [\varphi_{0,j,1} \mathbf{c}_{0,j,1}, \dots, \varphi_{0,j,K} \mathbf{c}_{0,j,K}]$ is the channel matrix between the mobiles of cell j and base station 0, $\mathbf{c}_{0,j,k}$ is the channel vector between base station 0 and cell j 's k -th mobile user and $(j) = (j \bmod Q)$. The variable \mathbf{W}_0 is i.i.d. $\mathcal{CN}(0, 1)$ and ϕ_τ is the average transmission power per mobile. The factor \sqrt{QK} guarantees that average power is ϕ_τ .

The received signal \mathbf{P}_0 is projected onto $\Psi_{0,k}$ in order to estimate $\mathbf{c}_{0,0,k}$ at the base station 0. After normalization, the resulting signals are

$$\bar{\mathbf{p}}_{0,k} = \mathbf{c}_{0,0,k} + \sum_{l \neq 0} \sqrt{\frac{\varphi_{0,lQ,k}}{\varphi_{0,0,k}}} \mathbf{c}_{0,lQ,k} + \frac{\mathbf{w}_{0,k}}{\sqrt{\varphi_{0,0,k} \phi_\tau KQ}} \in \mathbb{C}^{M \times 1}. \quad (3.4)$$

A minimum mean squared error (MMSE) estimator [42] is applied to the received vector of pilots to get

$$\hat{\mathbf{c}}_{0,0,k} = \mathbf{Y}_{cp} \mathbf{Y}_{pp}^{-1} \bar{\mathbf{p}}_{0,k}; \quad (3.5)$$

where \mathbf{Y}_{pp} and \mathbf{Y}_{cp} are the correlation and cross-correlation matrices, respectively. As all the channel vectors are independent therefore, the cross-correlation matrix becomes $\mathbf{Y}_{cp} = \mathbf{I}_M$. The correlation matrix \mathbf{Y}_{pp} is given as

$$\mathbf{Y}_{pp} = \mathbf{I}_M + \underbrace{\sum_{l \neq 0} \frac{\varphi_{0,lQ,k}}{\varphi_{0,0,k}} \mathbf{I}_M}_{a_1} + \underbrace{\frac{1}{\varphi_{0,0,k} \phi_\tau KQ} \mathbf{I}_M}_{a_2}. \quad (3.6)$$

From the above equation, we can define $\sigma_\tau^2 = (1 + a_1 + a_2)^{-1}$ and now applying the MMSE decomposition

$$\mathbf{c}_{0,0,k} = \hat{\mathbf{c}}_{0,0,k} + \tilde{\mathbf{c}}_{0,0,k}, \quad (3.7)$$

where $\tilde{\mathbf{c}}_{0,0,k}$ is the independent uncorrelated estimation error. Both the entries are i.i.d. where $\hat{\mathbf{c}}_{0,0,k}$ is $\mathcal{CN}(0, \sigma_\tau^2)$ and $\tilde{\mathbf{c}}_{0,0,k}$ is $\mathcal{CN}(0, 1 - \sigma_\tau^2)$.

3.1.2 Actual Transmission of Data

In the next $T - KQ$ slots, all the mobiles transmit their data. This takes place in all cells after the uplink training of pilots. The received signal at base station 0 is

$$\mathbf{r}_0 = \sum_{j,k} \sqrt{\phi \varphi_{0,j,k}} \mathbf{c}_{0,j,k} r_{j,k} + \mathbf{n}_0, \quad (3.8)$$

where ϕ is the average power consumed by a mobile to transmit the data $r_{j,k}$ by a user k in cell j and \mathbf{n}_0 is the noise, which is $\mathcal{CN}(0, 1)$. At base station 0, maximum ratio combining (MRC) is applied to receive the k -th mobile's signal. The unit norm vector is denoted as

$$\mathbf{u}_k = \frac{\hat{\mathbf{c}}_{0,0,k}}{\|\hat{\mathbf{c}}_{0,0,k}\|} \in \mathbb{C}^{M \times 1}. \quad (3.9)$$

After applying maximum ratio combining and normalization, we get

$$\mathbf{u}_k^* \bar{\mathbf{r}}_0 = \mathbf{u}_k^* \hat{\mathbf{c}}_{0,0,k} r_{0,k} + \sqrt{\frac{1}{\phi_\tau \varphi_{0,0,k}}} w_k \quad (3.10)$$

$$+ \mathbf{u}_k^* \tilde{\mathbf{c}}_{0,0,k} r_{0,k} + \mathbf{u}_k^* \sum_{i \neq k} \sqrt{\frac{\varphi_{0,0,i}}{\varphi_{0,0,k}}} \mathbf{c}_{0,0,i} r_{0,i} \quad (10a)$$

$$+ \mathbf{u}_k^* \sum_{j \neq 0} \sum_{i=1}^K \sqrt{\frac{\varphi_{0,j,i}}{\varphi_{0,0,k}}} \mathbf{c}_{0,j,i} r_{j,i}. \quad (10b)$$

In (3.10), the two terms are desired signal and the noise respectively. In (3.10a) the terms refer to intra-cell interference and in (3.10b) the term denotes inter-cell interference.

3.1.3 Achievable Cell Throughput

The average throughput of cell 0 using the above mentioned scheme is achieved by the following derivation. Tier-1 base stations of hexagonal geometry with

M -antenna are deployed. Each base station serves K randomly located single antenna mobiles of its own cell with path loss factor $\varphi_{0,0,k}$. The inter cell interference in equation (3.10b) can be re-written as

$$\begin{aligned} \mathbf{u}_k^* \sum_{j \neq 0} \sum_{i=1}^K \sqrt{\frac{\varphi_{0,j,i}}{\varphi_{0,0,k}}} \mathbf{c}_{0,j,i} r_{j,i} - \mathbf{u}_k^* \sum_{l \neq 0} \sqrt{\frac{\varphi_{0,lQ,k}}{\varphi_{0,0,k}}} \mathbf{c}_{0,lQ,k} r_{lQ,k} & \quad (3.11) \\ + \mathbf{u}_k^* \sum_{l \neq 0} \sqrt{\frac{\varphi_{0,lQ,k}}{\varphi_{0,0,k}}} \mathbf{c}_{0,lQ,k} r_{lQ,k}, & \quad (11a) \end{aligned}$$

where (3.11a) represents the pilot contamination. For a single user k , we can calculate the throughput as

$$\mathcal{R} \geq \log \left(1 + \frac{|\mathbf{u}_k^* \hat{\mathbf{c}}_{0,0,k}|^2}{\frac{1}{\phi \varphi_{0,0,k}} + I_1 + I_2 + I_3} \right), \quad (3.12)$$

where I_1 , I_2 , I_3 are intra-cell, inter-cell and interference due to pilot contamination, respectively and given as

$$I_1 = |\mathbf{u}_k^* \tilde{\mathbf{c}}_{0,0,k}|^2 + \sum_{i \neq k} \left| \mathbf{u}_k^* \sqrt{\frac{\varphi_{0,0,i}}{\varphi_{0,0,k}}} \mathbf{c}_{0,0,i} \right|^2, \quad (3.13)$$

$$I_2 = \sum_{j \neq 0} \sum_{i=1}^K \frac{\varphi_{0,j,i}}{\varphi_{0,0,k}} |\mathbf{u}_k^* \mathbf{c}_{0,j,i}|^2 - \sum_{l \neq 0} \frac{\varphi_{0,lQ,k}}{\varphi_{0,0,k}} |\mathbf{u}_k^* \mathbf{c}_{0,lQ,k}|^2, \quad (3.14)$$

$$I_3 = \sum_{l \neq 0} \frac{\varphi_{0,lQ,k}}{\varphi_{0,0,k}} |\mathbf{u}_k^* \mathbf{c}_{0,lQ,k}|^2. \quad (3.15)$$

Both the terms I_1 and I_2 are independent of $|\mathbf{u}_k^* \hat{\mathbf{c}}_{0,0,k}|^2$, whereas I_3 is dependent upon $\mathbf{c}_{0,0,k}$ which also shows dependence upon $|\mathbf{u}_k^* \hat{\mathbf{c}}_{0,0,k}|^2$. In order to analyze I_3 , MMSE decomposition is applied on $\mathbf{c}_{0,lQ,k}$. Hence we can write $\hat{\mathbf{c}}_{0,lQ,k}$ as $\hat{\mathbf{c}}_{0,0,k}$ because the MMSE decomposition for both the terms is proportional. Thus,

$$\mathbf{c}_{0,lQ,k} = \sqrt{\frac{\varphi_{0,lQ,k}}{\varphi_{0,0,k}}} \hat{\mathbf{c}}_{0,0,k} + \tilde{\mathbf{c}}_{0,lQ,k}, \quad (3.16)$$

where $\tilde{\mathbf{c}}_{0,lQ,k}$ is i.i.d. $\mathcal{CN}(0, 1 - \frac{\varphi_{0,lQ,k}}{\varphi_{0,0,k}} \sigma_\tau^2)$ and denotes the estimation error and is not dependent upon $\hat{\mathbf{c}}_{0,lQ,k}$. Re-write I_3 as

$$\begin{aligned} I_3 &= \sum_{l \neq 0} \frac{\varphi_{0,lQ,k}^2}{\varphi_{0,0,k}^2} |\mathbf{u}_k^* \hat{\mathbf{c}}_{0,0,k}|^2 + \sum_{l \neq 0} \frac{\varphi_{0,lQ,k}}{\varphi_{0,0,k}} |\mathbf{u}_k^* \tilde{\mathbf{c}}_{0,lQ,k}|^2 \\ &+ \sum_{l \neq 0} \left(\left(\frac{\varphi_{0,lQ,k}}{\varphi_{0,0,k}} \right)^{\frac{3}{2}} (\mathbf{u}_k^* \hat{\mathbf{c}}_{0,0,k} \tilde{\mathbf{c}}_{0,lQ,k}^* \mathbf{u}_k + \mathbf{u}_k^* \tilde{\mathbf{c}}_{0,lQ,k} \hat{\mathbf{c}}_{0,0,k}^* \mathbf{u}_k) \right), \end{aligned} \quad (3.17)$$

and denote the rate conditioned on $\hat{\mathbf{c}}_{0,0,k}^*$ by $\bar{\mathcal{R}}$. To achieve the lower bound of $\bar{\mathcal{R}}$, convexity of $\log(1 + \frac{1}{x})$ is used, therefore,

$$\bar{\mathcal{R}} \geq \log \left(1 + \frac{|\mathbf{u}_k^* \hat{\mathbf{c}}_{0,0,k}|^2}{\frac{1}{\phi \varphi_{0,0,k}} + \mathbb{E}[I_1] + \mathbb{E}[I_2] + \mathbb{E}[I_3]} \right) \quad (3.18)$$

where $\mathbb{E}[I_1]$, $\mathbb{E}[I_2]$ and $\mathbb{E}[I_3]$ are given as

$$\mathbb{E}[I_1] = (1 - \sigma_\tau^2) + \sum_{i \neq k} \frac{\varphi_{0,0,i}}{\varphi_{0,0,k}} \quad (3.19)$$

$$\mathbb{E}[I_2] = \sum_{j \neq 0} \sum_{i=1}^K \frac{\varphi_{0,j,i}}{\varphi_{0,0,k}} - \sum_{l \neq 0} \frac{\varphi_{0,lQ,k}}{\varphi_{0,0,k}} \quad (3.20)$$

$$\mathbb{E}[I_3] = \sum_{l \neq 0} \frac{\varphi_{0,lQ,k}^2}{\varphi_{0,0,k}^2} |\mathbf{u}_k^* \hat{\mathbf{c}}_{0,0,k}|^2 + \sum_{l \neq 0} \frac{\varphi_{0,lQ,k}}{\varphi_{0,0,k}} \left(1 - \frac{\varphi_{0,lQ,k}}{\varphi_{0,0,k}} \sigma_\tau^2 \right). \quad (3.21)$$

The last two terms in (20) have zero mean hence neglected in (24). Note that

$$|\mathbf{u}_k^* \hat{\mathbf{c}}_{0,0,k}|^2 = \sum_{q=1}^M \hat{c}_{k,q}^2, \quad (3.22)$$

where the term $\hat{c}_{k,q}$ is i.i.d. $\mathcal{CN}(0, \sigma_\tau^2)$. Hence, $|\mathbf{u}_k^* \hat{\mathbf{c}}_{0,0,k}|^2$ has Gamma distribution with parameters (M, σ_τ^2) . The right hand side of (21) is written as

$$\log \left(1 + \frac{\Gamma_k}{\frac{1}{\phi\varphi_{0,0,k}} + \Omega_1 + \Omega_2 + \sum_{l \neq 0} \frac{\varphi_{0,lQ,k}^2}{\varphi_{0,0,k}^2} \Gamma_k} \right), \quad (3.23)$$

where $\Gamma_k = |\mathbf{u}_k^* \hat{\mathbf{c}}_{0,0,k}|^2$, Ω_1 is the intra-cell interference and Ω_2 is the inter-cell interference given as

$$\Omega_1 = (1 - \sigma_\tau^2) + \sum_{i \neq k} \frac{\varphi_{0,0,i}}{\varphi_{0,0,k}}, \quad (3.24)$$

$$\Omega_2 = \sum_{j \neq 0} \sum_{i=1}^K \frac{\varphi_{0,j,i}}{\varphi_{0,0,k}} - \sum_{l \neq 0} \frac{\varphi_{0,lQ,k}^2}{\varphi_{0,0,k}^2} \sigma_\tau^2. \quad (3.25)$$

The inverse Gamma distribution ($1/\Gamma_k$) has a mean value of $1/(M-1)\sigma_\tau^2$ [43]. Therefore,

$$\mathcal{R}_k \geq \log \left(1 + \frac{1}{\left(\frac{1}{\phi\varphi_{0,0,k}} + \Omega_1 + \Omega_2\right)/\Gamma_k + \sum_{l \neq 0} \frac{\varphi_{0,lQ,k}^2}{\varphi_{0,0,k}^2}} \right) \quad (3.26)$$

$$\geq \log \left(1 + \frac{1}{\left(\frac{1}{\phi\varphi_{0,0,k}} + \Omega_1 + \Omega_2\right)/\mathbb{E} \left[\frac{1}{\Gamma_k} \right] + \sum_{l \neq 0} \frac{\varphi_{0,lQ,k}^2}{\varphi_{0,0,k}^2}} \right) \quad (3.27)$$

$$\geq \log \left(1 + \frac{(M-1)\sigma_\tau^2}{\left(\frac{1}{\phi\varphi_{0,0,k}} + \Omega_1 + \Omega_2 + \Omega_3\right)} \right) \quad (3.28)$$

where $\Omega_3 = (M-1) \sum_{l \neq 0} \frac{\varphi_{0,lQ,k}^2}{\varphi_{0,0,k}^2} \sigma_\tau^2$ is the pilot contamination.

The average achievable throughput for cell 0 is given by

$$\mathcal{R} \geq K \left(1 - \frac{QK}{T}\right) \log \left(1 + \frac{(M-1)\sigma_\tau^2}{\frac{1}{\phi\varphi_{0,0,k}} + \Omega_1 + \Omega_2 + \Omega_3} \right), \quad (3.29)$$

where ϕ is the average data power, T is the channel coherence period and σ_τ^2 is the normalized estimation power

$$\sigma_\tau^2 = \left(1 + \sum_{l \neq 0} \frac{\varphi_{0,lQ,k}}{\varphi_{0,0,k}} + \frac{1}{\sqrt{\phi_\tau K Q}} \right)^{-1}. \quad (3.30)$$

In (29) the constants Ω_1 , Ω_2 and Ω_3 are defined as

$$\begin{aligned} \Omega_1 &= (1 - \sigma_\tau^2) + \sum_{i \neq k} \frac{\varphi_{0,0,i}}{\varphi_{0,0,k}}, \\ \Omega_2 &= \sum_{j \neq 0} \sum_{i=1}^K \frac{\varphi_{0,j,i}}{\varphi_{0,0,k}} - \sum_{l \neq 0} \frac{\varphi_{0,lQ,k}^2}{\varphi_{0,0,k}^2} \sigma_\tau^2, \\ \Omega_3 &= (M - 1) \sigma_\tau^2 \sum_{l \neq 0} \frac{\varphi_{0,lQ,k}^2}{\varphi_{0,0,k}^2}. \end{aligned} \quad (3.31)$$

The derived equation for cell throughput \mathcal{R} is valid for even small values of M and the achievable rate is *non-asymptotic* which is valid for any M . Three types of interference terms are characterized in this derivation, Ω_1 is the intra-cell interference, Ω_2 is the inter-cell interference and Ω_3 is the interference caused due to pilot contamination. Ω_2 is referred as *non-coherent interference* whereas Ω_3 is the coherently added inter-cell interference referred as *coherent interference*. Both Ω_1 and Ω_2 have direct dependence upon K but are independent of M . Both these interferences also depend upon the network topology, if the cell size is large then less inter and intra-cell interference will occur keeping other parameters constant. Whereas, Ω_3 increases linearly with M and is independent of K as there is only single mobile per cell that is using the pilot with same frequency.

Chapter 4

Numerical Results

In this section, we evaluate the effect of different interferences, pilot reuse factor and network topology on the average cell throughput. Different simulations have been carried out to study the parameters upon which maximum throughput is achieved. For all simulations, we assume coherence period $T = 100\text{ms}$, radius $R = 1.4\text{km}$, path loss exponent $\alpha = 3.8$ and $\phi_\tau = \phi = 100\text{mW}$, unless noted otherwise. All the mobiles operate at 3GHz frequency and 10MHz bandwidth. In order to get ergodic cell throughput, *Monte-Carlo* method is applied with $1e6$ simulations for a single user having random location in every trial.

Fig. 2 shows the average throughput of the system versus the number of users. We can observe the dependence of throughput on the reuse factor and the number of users per cell. Average throughput of a cell increases when the number of users increases. Similarly \mathcal{R} increases as the reuse factor goes from 1 to 7 because the *coherent interference* decreases when the interfering mobiles get far away from the serving cell 0's base station. On the contrary, *Non-coherent* and intra-cell interference have no effect with the

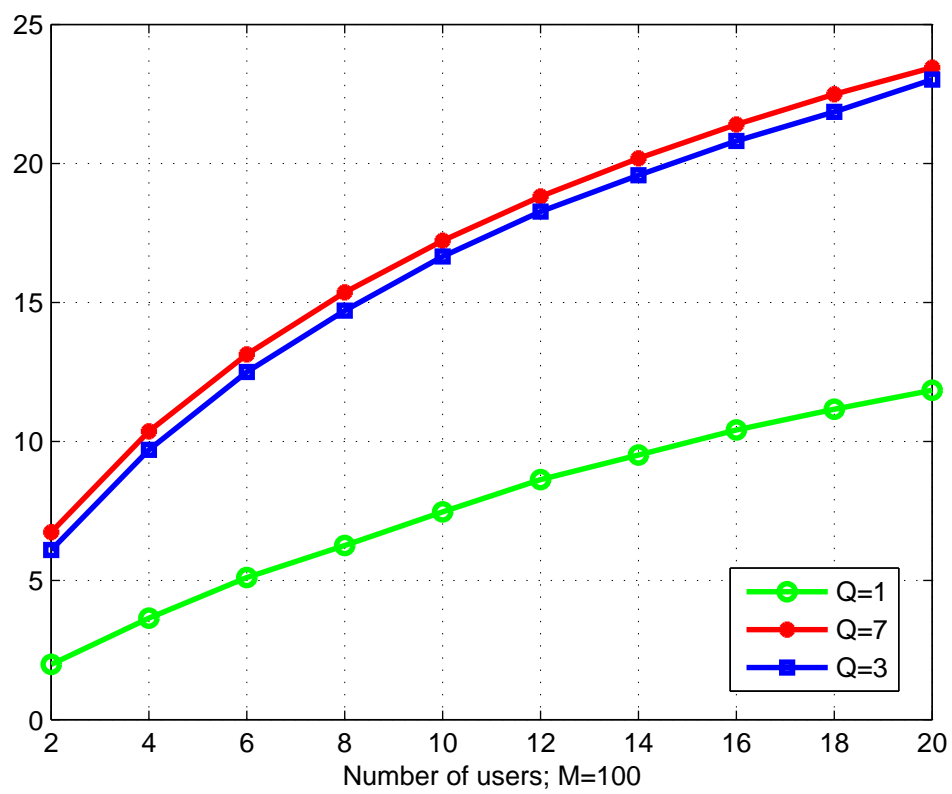


Figure 4.1: Average throughput with different number of users and reuse factor

change in Q but both interferences tend to increase with increasing K . The gain overcomes the loss due to both interferences hence the final net result is the increase in average throughput of a cell. Fig. 2 also shows the achievable throughput to a specific number of users for different reuse factors. For example, a throughput of more than 20 bits/sec/Hz is provided when serving 20 users for $Q=3$.

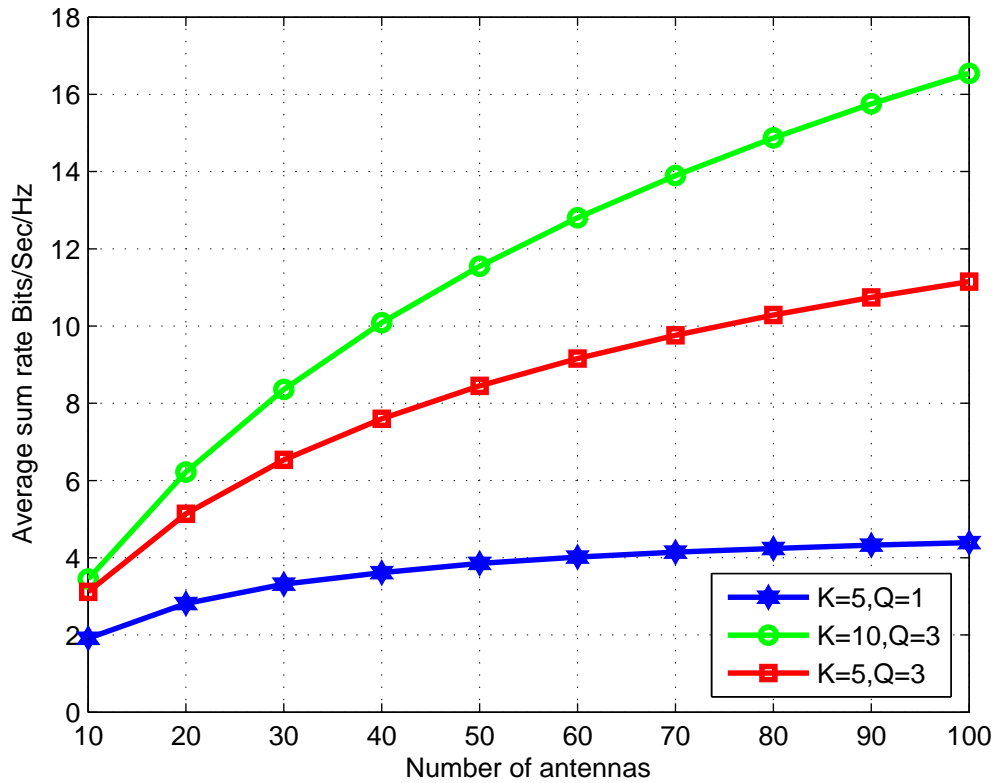


Figure 4.2: Average throughput with different number of antennas

Fig. 3 depicts the relation between number of antennas and the average throughput for different reuse factor. The average sum-rate increases as the number of antennas increase. The saturation in throughput is not obvious

for 100 antennas for reuse factor 3 as the interference power caused by pilot contamination using $Q=3$ is very small, whereas, the throughput saturates for higher number of antennas at reuse factor 1. Hence we can say that pilot contamination almost vanishes for higher reuse factors.

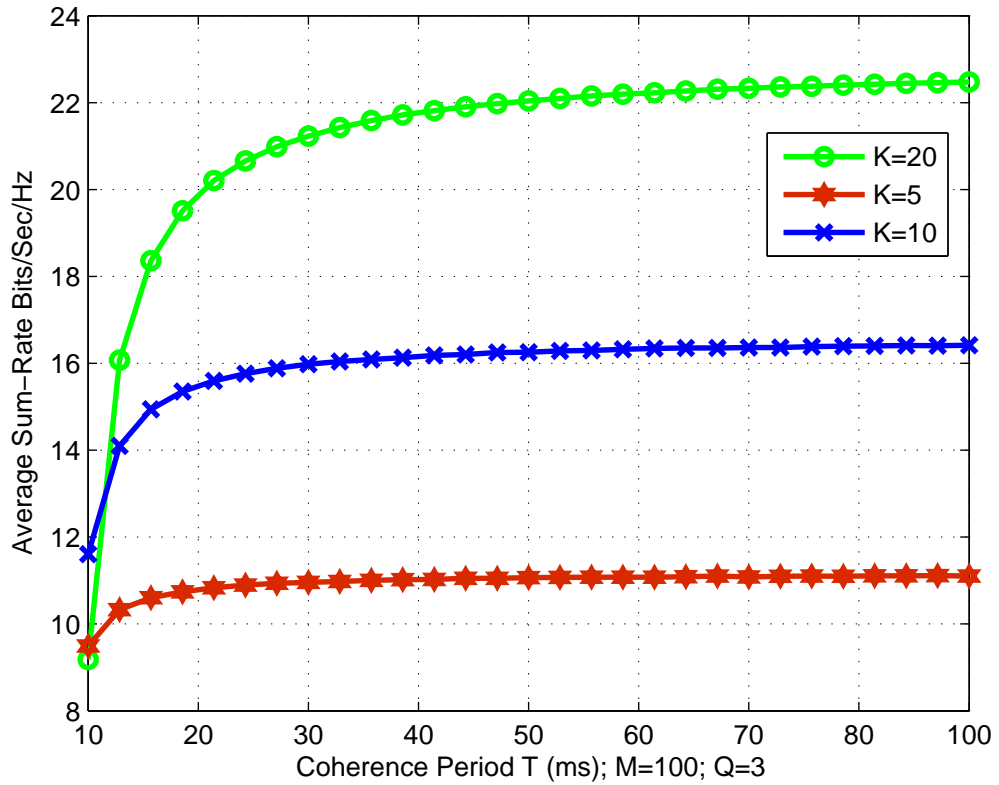


Figure 4.3: Average throughput with coherence period and different number of users

Fig. 4 shows the relation between coherence period T and the average throughput with different number of mobiles K . When we consider only 5 users in a cell, the throughput doesn't change much with the increase in T but when K goes to 20, the throughput starts increasing gradually as T

increases. It can be seen that for lower T , $K=20$ has the least performance. This is because, it is very difficult to generate orthogonal pilots for more users in lesser coherence period and hence the pilot contamination dominates the system. When T increases beyond a specific value, $K=20$ outperforms the rest of two cases.

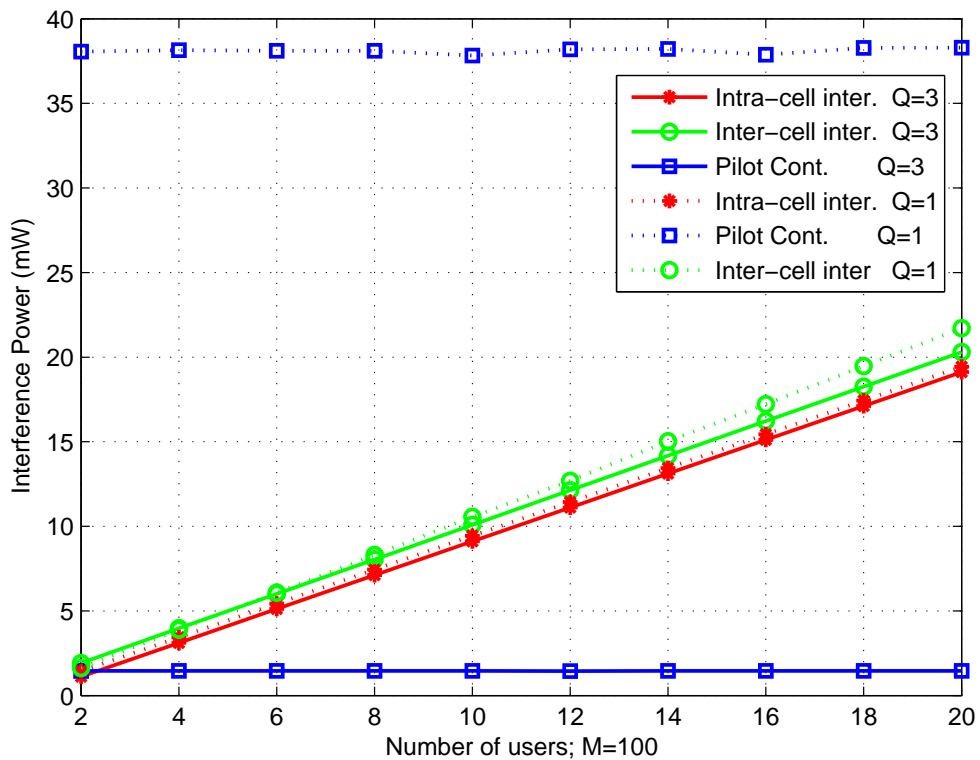


Figure 4.4: Interference types with reuse factor and different number of users

Fig. 5 shows the dependence of different interference components upon the reuse factor and the number of users. As the number of users increases the inter-cell and intra-cell interference increase, whereas, the pilot contamination stays constant because for tier-1, the number of interferers causing

pilot contamination will always be six for any reuse factor. On the average, the inter-cell and intra-cell interferences have the same impact on the throughput because the location of user is random; for distances closer to the base station, the intra-cell interference dominates and for distances far away, the inter-cell interference dominates. Hence, on the average, both contribute the same to the cell throughput. It can also be observed from Fig. 5 that the reuse factor only affects the pilot contamination, whereas, the inter-cell and intra-cell interferences remain almost constant because the interferers that cause pilot contamination move away from the serving cell as the reuse factor increases. Hence, the throughput is increased while using higher reuse factors.

Fig. 4.5 shows the average throughput rates for two receivers i.e. MMSE and MRC. We can see that MMSE receiver performs better than the MRC for all number of antennas. This is because of the reason that MMSE minimizes the interference terms only, whereas, MRC amplifies the whole signal and then multiplies the data that has higher amplitude with some weights of higher value and leaves the low amplitude signals as it is that does not ensure the minimization of interference. In MMSE receivers the interference terms are minimized to zero and the original data is amplified. Hence, we get higher rates in case of MMSE receiver.

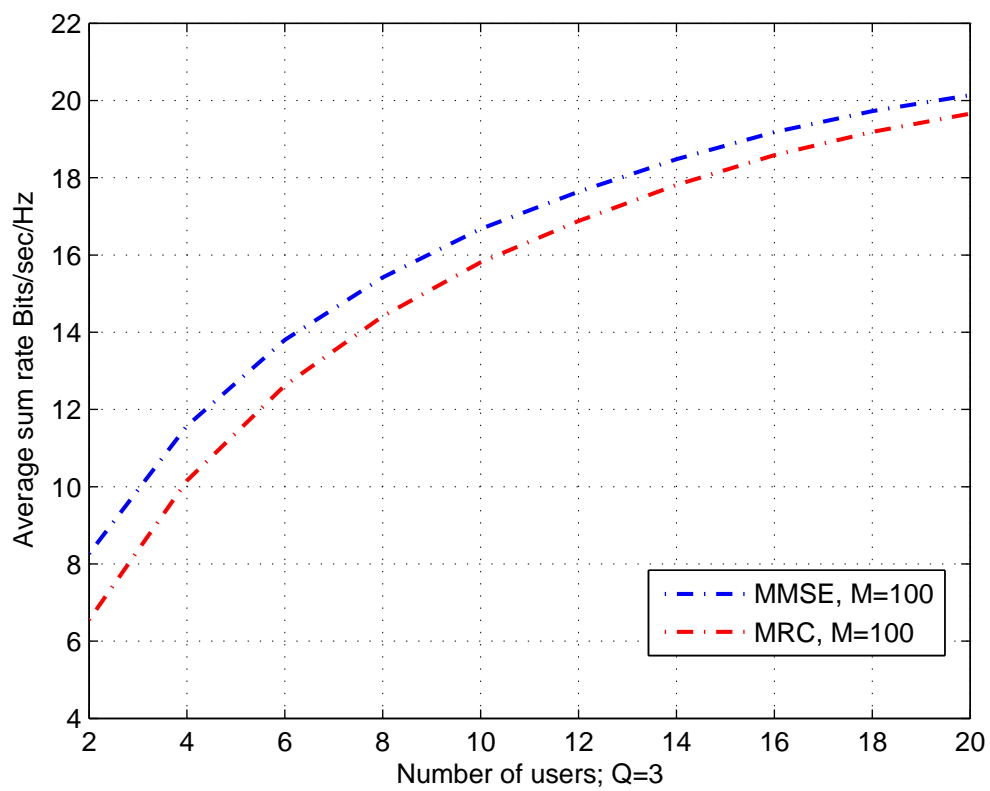


Figure 4.5: Comparison between throughputs of MMSE and MRC receivers

Chapter 5

Conclusion

In this paper, we evaluated the lower bound for non-asymptotic throughput of an uplink massive MIMO system with hexagonal geometry and random deployment of users. It was observed that the effect of pilot contamination diminishes when we have reuse factor greater than 1. Moreover, relationship between the number of users in a cell, number of base station antennas, duration of coherence period and average cell throughput has been studied through simulations. Through these studies, we can calculate the lower bound of average throughput for a cell that can be achieved for the different values of parameters like K, T, Q and M . We quantified the cell throughput for various reuse factors and showed that by moving to higher reuse factors, pilot contamination is reduced, however, there is very little or no effect on the inter-cell and intra-cell interference. We considered only MRC receivers, however in future we intend to also look into the MMSE receivers.

Bibliography

- [1] F. Rusek, D. Persson, B. K. Lau, E. G. Larsson, T. L. Marzetta, O. Edfors, and F. Tufvesson, "Scaling up MIMO: Opportunities and challenges with very large arrays," *IEEE Signal Process. Mag.*, vol. 30, pp. 4060, Jan. 2013.
- [2] H. Q. Ngo, E. G. Larsson, and T. L. Marzetta, "Energy and spectral efficiency of very large multiuser MIMO systems," *IEEE Trans. Commun.*, vol. 61, pp. 14361449, Apr. 2013.
- [3] B. Hochwald and T. Marzetta, "Adapting a downlink array from uplink measurements," *IEEE Trans. Signal Process.*, vol. 49, no. 3, pp. 642653, Mar 2001.
- [4] E. Larsson, O. Edfors, F. Tufvesson, and T. Marzetta, "Massive MIMO for next generation wireless systems" *IEEE Commun. Mag.*, vol. 52, no. 2, pp. 186195, Feb. 2014
- [5] T. Marzetta, "Noncooperative cellular wireless with unlimited numbers of base station antennas," *IEEE Trans. Wireless Commun.*, vol. 9, no. 11, pp. 35903600, Sep. 2010.

- [6] M. Jain, J. Choi, T. Kim, D. Bharadia, S. Seth, K. Srinivasan, P. Levis, S. Katti, and P. Sinha, "Practical, real-time, full duplex wireless," in *Proc. Int. Conf. on Mobile Computing and Networking (ACM)*, New York, NY, USA, 2011, pp. 301312.
- [7] D. Chizhik, F. Rashid-Farrokhi, J. Ling, and A. Lozano, "Effect of antenna separation on the capacity of BLAST in correlated channels," *IEEE Commun. Lett.*, vol. 4, no. 11, pp. 337339, Nov. 2000.
- [8] J. Duplicy, B. Badic, R. Balraj, R. Ghaffar, P. Horvath, F. Kaltenberger, R. Knopp, I. Kovacs, H. Nguyen, D. Tandur, and G. Vivier, "MU-MIMO in LTE systems," *EURASIP J. on Wireless Comm. and Netw.*, Mar. 2011.
- [9] C. Shepard, H. Yu, N. Anand, L. E. Li, T. L. Marzetta, R. Yang, and L. Zhong "Argos: Practical many-antenna base stations," *ACM Int. Conf. Mobile Computing and Networking (MobiCom)*, 2002.
- [10] F. Kaltenberger, J. Haiyong, M. Guillaud, and R. Knopp, "Relative channel reciprocity calibration in MIMO/TDD systems," *Proc. of Future Network and Mobile Summit, 2010*, 2002.
- [11] B. Gopalakrishnan and N. Jindal, "How much training is required for multiuser MIMO?" in *Proc. IEEE Workshop on Signal Processing Adv. in Wire-less Commun. (SPAWC)*, Jun 2011, pp. 381385.
- [12] F. Rusek, D. Persson, B. K. Lau, E. G. Larsson, T. L. Marzetta, O. Edfors, and F. Tufves-son, "Scaling up MIMO: Opportunities and challenges

- with very large arrays,” *IEEE Commun. Mag.*, Jan. 2013., vol.54, pp. 1268-1278,
- [13] N. Krishnan, R. Yates, , and N. Mandayam, “Uplink linear receivers for multicell multiuser MIMO with pilot contamination: Large system analysis,” *IEEE Trans. Wireless Commun.*, vol. 13, no. 8, pp. 4360-4373, Aug. 2014.
- [14] E. Dahlman, S. Parkvall, and J. Skold, “4G: LTE/LTE-Advanced for Mobile Broadband”.*Elsevier*, 2014.
- [15] M. Biguesh and A. Gershman, “Training-based mimo channel estimation: a study of estimator tradeoffs and optimal training signals,” *IEEE Trans. Signal Process.*, vol. 54, no. 3, pp. 884-893, Mar 2006.
- [16] J. Jose, A. Ashikhmin, T. Marzetta, and S. Vishwanath, “Pilot contamination problem in multi-cell TDD systems,” in *Proc. IEEE Int. Symp. on Inf. Theory (ISIT)*, Jun 2009, pp. 2184-2188.
- [17] H. Yin, D. Gesbert, M. Filippou, and Y. Liu, “A coordinated approach to channel estimation in large-scale multiple-antenna systems,” *IEEE J. Sel. Areas Commun.*, vol. 31, no. 2, pp. 264-273, Feb 2013.
- [18] T. L. Marzetta “Noncooperative cellular wireless with unlimited number of base station antenna,” *IEEE Trans. Wireless Commun.*, vol. 9, no. 11, pp. 3590-3600, Nov. 2010.
- [19] A. Ashikhmin and T. L. Marzetta “Pilot contamination precoding in multi-cell large scale antenna systems,” *IEEE International Symposium on Information Theory (ISIT)*, Cambridge, MA, Jul. 2012

- [20] A. Paulraj, R. Nabar, and D. Gore, "Introduction to Space-Time Wireless Communications". *Cambridge University Press*, 2008
- [21] G. Xiang, F. Tufvesson, O. Edfors, and F. Rusek, "Measured propagation characteristics for very-large MIMO at 2.6 GHz," in *Proc. IEEE Asilomar Conf. Signals, Systems, and Computers*, Nov. 2012, pp. 295299.
- [22] M. Steinbauer, A. Molisch, and E. Bonek, "The double-directional radio channel," *IEEE Anten. and Prop. Mag.*, vol. 43, no. 4, pp. 5163, Aug. 2001.
- [23] ITU-R, "Guidelines for evaluation of radio interface technologies for IM-TAdvanced," *International Telecommunication Union*, Tech. Rep. ITU-R, M.2135-1, Dec. 2009.
- [24] T. L. Marzetta and B. M. Hochwald, "Fast transfer of channel state information in wireless systems," *IEEE Trans. Signal Process.*, vol.54, pp. 1268-1278, 2006.
- [25] L. Lu, G. Y. Li, A. L. Swindlehurst, A. Ashikhmin, and R. Zhang, "An overview of massive MIMO: Benets and challenges," *IEEE J. Sel Topics Signal Process.*, April 2014.
- [26] J. Jose, A. Ashikhmin, T. L. Marzetta and S. Vishwanath. "Pilot contamination problem in multi-cell TDD systems," *IEEE International Symposium on Information Theory*, pp 2184-2188, July, 2009.
- [27] B. Gopalkrishnan and N. Jindal, "An analysis of pilot contamination on Multi-user MIMO cellular systems with many antennas," *IEEE SPAWC*, pp. 381-385, June 2011.

- [28] H. Q. Ngo, T.L.Marzetta and E.G.Larsson “Analysis of pilot contamination effect in very large multicell multiuser MIMO systems for physical channel models”, *IEEE ICASSP*, pp. 3464-3467, May 2011.
- [29] T. E. Bogale and L. B. Le “Pilot optimization and channel estimation for multiuser massive MIMO systems”, *IEEE CISS*, Mar. 2014.
- [30] Papadopoulos, G. Caire and S. Ramprashad, “Achieving large spectral efficiencies from MU-MIMO with tens of antennas: location adaptive TDD MU-MIMO design and user scheduling”, *IEEE ASILOMAR*, pp. 636-643, Nov. 2010.
- [31] H. Huh, G. Caire, Papadopoulos, Ramprashad “Achieving ”Massive MIMO” Spectral Efficiency with a Not-so-Large Number of Antennas,” *IEEE Trans. on Wireless Communications*, vol.11, no.9, pp.3226-3239, September 2012
- [32] K. Appaiah, A. Ahsikhmin and T. Marzetta, “Pilot contamination reduction in multi-user TDD systems,” *IEEE ICC*, May 2010.
- [33] P. Xu, J. Wang and J. Wang “Effect of pilot contamination on channel estimation in massive MIMO systems,” *IEEE WCSP*, 2013.
- [34] S. M. Kay, “Fundamentals of statistical signal processing: estimation theory”. *Prentice-Hall*, 1993.
- [35] H. Yin, D. Gesbert, M. Filippou, and Y. Liu, “A coordinated approach to channel estimation in large-scale multiple-antenna systems,” *IEEE J. Sel. Areas Commun.*, vol. 31, no. 2, pp. 264273, Feb 2013.

- [36] Y. Li, Y.-H. Nam, B. I. Ng and J. Zhang “A non-asymptotic throughput for massive MIMO cellular uplink with pilot reuse,” *Wireless Communication Symposium - Globecom*, pp. 4500-4504, 2012.
- [37] P. Xu, J. Wang, and J. Wang, “Effect of pilot contamination on channel estimation in massive MIMO systems,” in *Proc. Int. Conf. on Wireless Commun. Signal Proces. (ICWCSP)*, Oct 2013, pp. 16.
- [38] A. Simonsson and A. Furuskar, “Uplink power control in LTE - overview and performance,” in *Proc. IEEE Veh. Tech. Conf. (VTC)*, Sep 2008, pp. 15.
- [39] A. Scherb and K. Kammeyer, “Bayesian channel estimation for doubly correlated mimo systems,” in *Proc. ITG Workshop on Smart Antennas (WSA)*, Vienna, Austria, Feb 2007.
- [40] M. Frenne, “On RSRP determination for UE to node association,” *3rd Generation Partnership Project, Tech. Rep. 3GPP, TSG-RAN WG1 Meeting 75*, Aug. 2001.
- [41] S. Jrmyr, “MIMO transceiver design for multi-antenna communications over fading channels,” *Ph.D. dissertation, Royal Institute of Technology (KTH)*, Sweden, 2013.
- [42] G. L. Stuber, *Principles of Mobile Communication*, 2nd ed. NYC, NY, USA: Springer, 2011.
- [43] David G. T. Denison, Christopher C. Holmes, Bani K. Mallick, Adrian F. M. Smith *Bayesian Methods for Nonlinear Classification and Regression*, 2002.